Journal of Sound and Vibration (2001) **241**(2), 271–281
doi:10.1006/jsvi.2000.3294, available online at http://www.idealibrary.com on IDEAL®

A NEW X-ACTUATOR DESIGN FOR DUAL BENDING/TWISTING CONTROL OF WINGS

H. S. Tzou

Department of Mechanical Engineering, StrucTronics Laboratory, University of Kentucky, Lexington, KY 40506-0108, *U.S.A. E-mail: hstzou@engr.uky.edu*

R. Ye

Sealing Systems, Federal-Mogul Corporation, Ann Arbor, MI 48108, *U.S.A.*

AND

J. H. Ding

Department of Mechanical Engineering, StrucTronics Laboratory, University of Kentucky, Lexington, KY 40506-0108, *U.S.A.*

(*Received* 1 *October* 1999, *and in final form* 7 *August* 2000)

Recent development of smart structures and structronic systems has demonstrated the technology in many engineering applications. Active structural control of aircraft wings or helicopter blades (e.g., shapes, flaps, leading and/or trailing edges) can significantly enhance the aerodynamic efficiency and flight maneuverability of high-performance airplanes and helicopters. This paper is to evaluate the dual bending and torsion vibration control effects of an X-actuator configuration reconfigured from a parallel configuration. The finite element (FE) formulation of a new FE using the layerwise constant shear angle theory is reviewed and the derived governing equations are discussed. Bending and torsion control effects of plates are studied using the FE method and also demonstrated via laboratory experiments. The FE and experimental results both suggest the X-actuator is effective for both bending and torsion control of plates.

1. INTRODUCTION

Smart structures and structronics technology has been increasingly explored and gradually applied to engineering systems in recent years [1]. This technology emphasizes a true synergistic integration of structures and mechatronic/structronic systems with smart materials serving as *in situ* sensors, actuators, and/or elastic components in the design process. This synergistic integration can significantly simplify the system complexity and also improve the performance of next-generation precision machines, structures, mechatronic and structronic systems [2, 3].

Counteracting and controlling transverse bending vibration of wing or blade structures can reduce structural fatigue and thus enhance the reliability and service-life. Twisting airplane wings can effectively enhance the airplanes turning capability and flight maneuverability. (Flying birds inherently adopt this capability in natural environment.) Conventional actuator configuration applies parallel layouts of distributed actuators which are effective in controlling the bending oscillations and ineffective in controlling the twisting

0022-460X/01/120271 + 11 $35.00/0

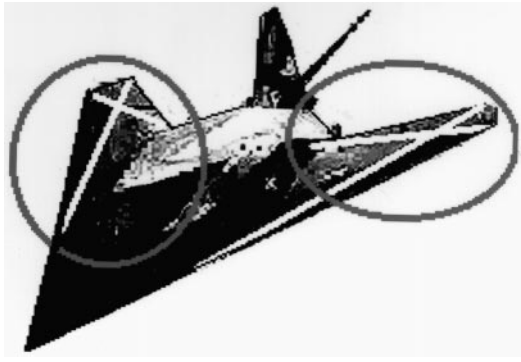

Figure 1. Wings with new X-actuators.

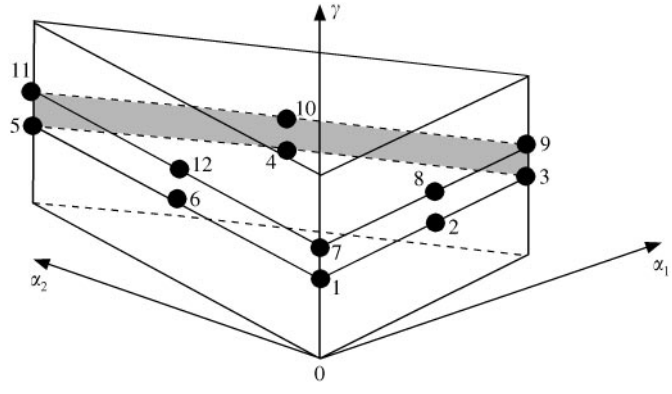

Figure 2. A triangular piezoelectric shell FE.

or torsional oscillations. Thus, a new design configuration with diagonally arranged piezoelectric actuator patches, the X-actuator configuration, is proposed (Figure 1). The vibration control effectiveness of the X-actuator configuration is studied using a newly developed finite element (FE) code and also demonstrated in laboratory experiments in this study.

The modern FE technique provides the utility and versatility in modeling, simulation, and analysis of various engineering designs. Thus, the FE method is used for analyzing and evaluating the two different actuator configurations. Isoparametric piezoelectric hexahedron and tetrahedron FEs were developed for piezoceramic transducer designs [4, 5]. Obal [6] used a piezoelectric beam FE in distributed vibration control of PZT-steel laminated beams. Tzou and Tseng [7] developed a non-conforming thin piezoelectric hexahedron FE with three internal degree-of-freedom (d.o.f.s) and applied it to the distributed sensing and vibration control of layered plates. Ha *et al.* [8] derived an 8-node composite brick element. Hwang and Park [9] developed a piezoelectric plate element and compared their results with published data. Rao and Sunar [10] proposed a thermopiezoelectric element. Tzou and Ye also derived a three-dimensional (3-D) thin piezothermoelastic element [11] and a triangular shell element [12], and examined the piezothermoelasticity and control effects of piezoelectric systems [13]. This paper is concerned with an application of a newly developed laminated quadratic C^0 piezoelastic triangular shell FE. The FE formulation of a laminated piezoelastic shell FE based on the

layerwise constant shear angle theory is briefly discussed. The FE analysis of the new X-actuator configuration is presented. Furthermore, an experimental model is fabricated and its bending/torsion control effectiveness is evaluated in this study.

2. FE FORMULATION

Fundamental piezoelectric constitutive equations are reviewed and introduction of FE formulation is presented in this section. The constitutive strain (S_{ij}) and electric field (E_i) equations of a piezoelectric continuum can be defined in generic tensor expressions [13]:

$$T_{ij} = c_{ijkl}S_{kl} - e_{mij}E_m, \quad D_n = e_{nkl}S_{kl} + \varepsilon_{nm}E_m, \tag{1, 2}$$

$$S_{ij} = (u_{i,j} + u_{j,i})/2, \quad E_i = -\phi_{,i}, \tag{3, 4}$$

where T_{ij} are the stresses, c_{ijkl} are the elastic moduli, e_{nkl} are the piezoelectric coefficients, D_n is the electric displacement, ε_{nm} are the dielectric constants or permittivities, u_i are the displacements, and ϕ is the electric potential [11–14]. The first equation denotes the induced stress as a function of the electric field in control applications; the second equation indicates the electric charge as a function of induced strain in sensor applications.

The FE formulation is based on the electromechanical coupling of piezoelectricity, emphasizing distributed sensing and control of structures. The layerwise constant shear angle theory is used in the shell FE formulation. A quadratic C^0 piezoelastic triangular shell u_{α_1}, u_{α_2} FE with twelve nodes, 4-d.o.f.s (u_{α_1}, u_{α_2} w, ϕ) per node, is derived. The element is quadratic in the two in-plane axes and linear in the transverse direction. The ith layer triangular element is bounded by the ith and $(i+1)$th interfaces; the interface triangle is characterized by 6 nodes, three at triangular corners and three at the centers of three sides on the interface plane parallel to the α_1–α_2 plane (Figure 2).

Thus, the displacement and electric fields $u_{(i)}(\zeta)$, $u_{(j)}(\zeta)$, $w_{(i)}(\zeta)$, and $\phi_{(i)}(\zeta)$ for the arbitrary ith layer can be expressed as

$$u_{\alpha_1}^{(i)}(\varsigma) = \mathbf{u}_{\alpha_1}^{(i)}(1 - \varsigma/h_i) + \mathbf{u}_{\alpha_1}^{(i+1)}(\varsigma/h_i), \tag{5}$$

$$u_{\alpha_2}^{(i)}(\varsigma) = \mathbf{u}_{\alpha_2}^{(i)}(1 - \varsigma/h_i) + \mathbf{u}_{\alpha_2}^{(i+1)}(\varsigma/h_i), \tag{6}$$

$$w^{(i)}(\varsigma) = \mathbf{w}^{(i)}(1 - \varsigma/h_i) + \mathbf{w}^{(i+1)}(\varsigma/h_i), \tag{7}$$

$$\phi^{(i)}(\varsigma) = \boldsymbol{\phi}^{(i)}(1 - \varsigma/h_i) + \boldsymbol{\phi}^{(i+1)}(\varsigma/h_i), \tag{8}$$

or simply written as

$$\{\mathbf{u}^{(i)}(\varsigma)\} = [N_u^{(i)}(\varsigma)] \cdot \{\mathbf{u}^{(i)}\}, \tag{9}$$

$$\{\phi^{(i)}(\varsigma)\} = [N_\phi^{(i)}(\varsigma)] \cdot \{\boldsymbol{\phi}^{(i)}\}, \tag{10}$$

where $\{\mathbf{u}^{(i)}\} = \{\mathbf{u}_{\alpha_1}^{(i)}, \mathbf{u}_{\alpha_2}^{(i)}, \mathbf{w}^{(i)}, \mathbf{u}_{\alpha_1}^{(i+1)}, \mathbf{u}_{\alpha_2}^{(i+1)}, \mathbf{w}^{(i+1)}\}$ is the displacement vector and $\{\boldsymbol{\phi}^{(i)}\} = \{\boldsymbol{\phi}^{(i)}, \boldsymbol{\phi}^{(i+1)}\}$ is the electric potential vector of the ith and $(i+1)$th interfaces along the curvilinear co-ordinate axes; $[N_u^{(i)}(\varsigma)]$ and $[N_\phi^{(i)}(\varsigma)]$ are the shape functions in terms of the co-ordinate ζ; and h_i is the thickness of the ith layer. Note that the co-ordinate ζ is local to

each layer. Furthermore, one can derive the nodal governing equations of the *j*th (planar) layer element located in the *i*th (thickness) layer in a matrix representation:

$$\begin{bmatrix} [M^{(i)}_{uu_j}] & 0 \\ 0 & 0 \end{bmatrix} \begin{Bmatrix} \{\ddot{u}^{(i)}_j\} \\ \{\ddot{\phi}^{(i)}_j\} \end{Bmatrix} + \begin{bmatrix} [C^{(i)}_{uu_j}] & 0 \\ 0 & 0 \end{bmatrix} \begin{Bmatrix} \{\dot{u}^{(i)}_j\} \\ \{\dot{\phi}^{(i)}_j\} \end{Bmatrix} + \begin{bmatrix} [K^{(i)}_{uu_j}] & [K^{(i)}_{u\phi_j}] \\ [K^{(i)}_{\phi u_j}] & [K^{(i)}_{\phi\phi_j}] \end{bmatrix} \begin{Bmatrix} \{u^{(i)}_j\} \\ \{\phi^{(i)}_j\} \end{Bmatrix} = \begin{Bmatrix} \{F^{(i)}_{u_j}\} \\ \{F^{(i)}_{\phi_j}\} \end{Bmatrix}, \tag{11}$$

where $[M_{uu}]$ is the mass matrix, $[C_{uu}]$ is the damping matrix, $[K_{uu}]$, $[K_{u\phi}]$, $[K_{\phi u}]$, and $[K_{\phi\phi}]$ are the stiffness matrices defined for the displacement and electric potential fields, and $\{F_u\}$ and $\{F_\phi\}$ are the mechanical and electrical excitations respectively. Based on the nodal equation, one can assemble the element matrices to yield the global system matrices:

$$\begin{bmatrix} [M_{uu}] & 0 \\ 0 & 0 \end{bmatrix} \begin{Bmatrix} \{\ddot{u}_j\} \\ \{\ddot{\phi}_j\} \end{Bmatrix} + \begin{bmatrix} [C_{uu}] & 0 \\ 0 & 0 \end{bmatrix} \begin{Bmatrix} \{\dot{u}_j\} \\ \{\dot{\phi}_j\} \end{Bmatrix} + \begin{bmatrix} [K_{uu}] & [K_{u\phi}] \\ [K_{\phi u}] & [K_{\phi\phi}] \end{bmatrix} \begin{Bmatrix} \{u_j\} \\ \{\phi_j\} \end{Bmatrix} = \begin{Bmatrix} \{F_u\} \\ \{F_\phi\} \end{Bmatrix}. \tag{12}$$

In general, the control force is introduced in the force vector $\{F_\phi\}$ which can be set up based on various control algorithms, such as the proportional feedback, the Lyapunov feedback, etc. [15]. Distributed control and sensing of distributed systems can be formulated afterwards. In this study, the negative velocity, proportional feedback is used to evaluate the two actuator configurations: (1) the parallel-actuator and (2) the X-actuator laminated on wing structures.

3. FE MODELLING AND ANALYSIS

To investigate the bending and torsion control effectiveness of wing panels, a FE plate model consisting of an elastic plate and piezoelectric control patches is studied. Note that the plate dimensions are specifically selected such that the first mode is the bending mode and the second mode is the torsion mode, although the first few natural modes of most aircraft wings are usually bending modes. Figure 3(a) and 3(b) illustrates the FE models laminated with a number of diagonally or parallelly aligned piezoelectric patches serving as distributed sensors and actuators. Note that the diagonally aligned actuator configuration

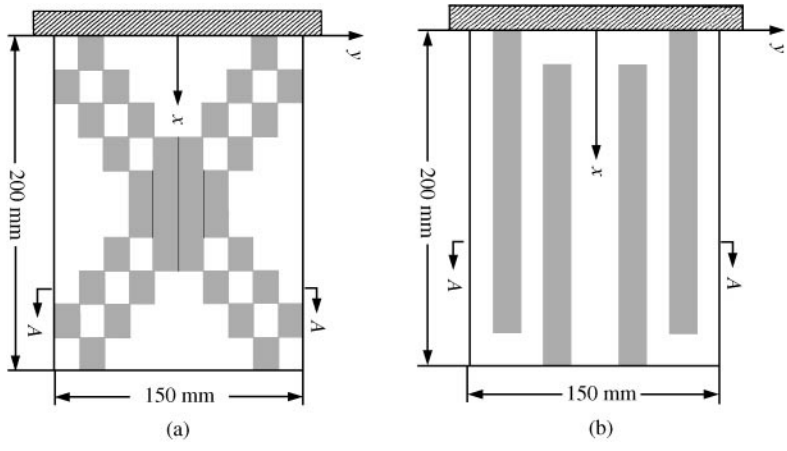

Figure 3. (a) Diagonal and (b) parallel configurations of the distributed actuators.

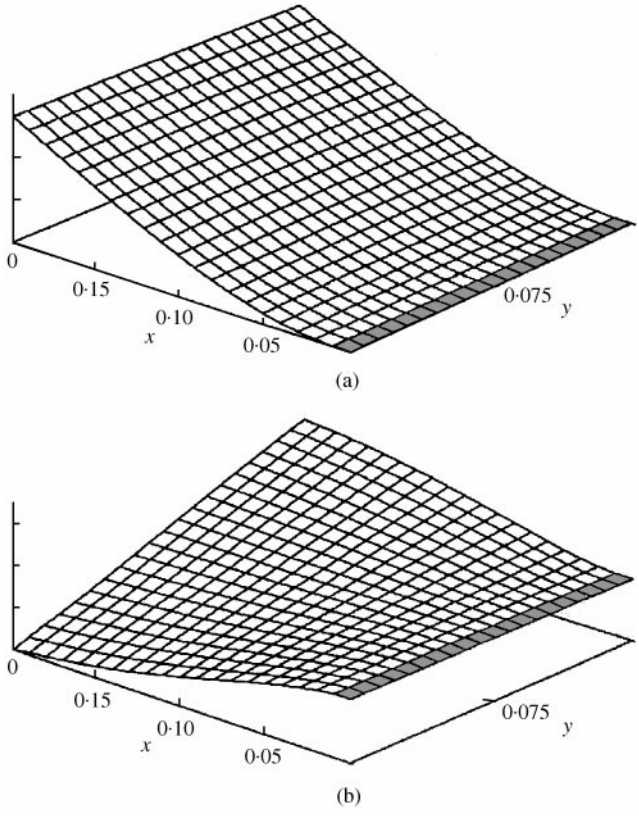

Figure 4. (a) Plate bending (1st plate mode) and (b) torsion (2nd plate mode) modes.

has the identical total actuator area as that of the parallel configuration. Figure 4(a) and 4(b) shows the first plate bending mode and the first torsion mode (the second plate mode).

3.1. CONTROL OF BENDING MODE

The snap-back free and controlled responses of the plate bending mode are presented in Figures 5–7. Note that both parallel and diagonal configurations provide identical bending control effects. These time histories clearly show the effectiveness of the negative proportional feedback control at various gains. Besides, comparing the above three snap-back responses suggests that both configurations are effective for bending mode control.

3.2. CONTROL OF TORSION MODE

Furthermore, snap-back free and controlled torsion vibrations are also presented in Figures 8–10. Recall that the parallel actuator configuration is only effective to control the bending oscillations (Figures 6 and 7) and ineffective for any torsion oscillations. However, the new X-configuration is effective for both bending and torsion vibrations, as shown in Figures 5–10. FE simulation results prove that the parallel and diagonal configurations

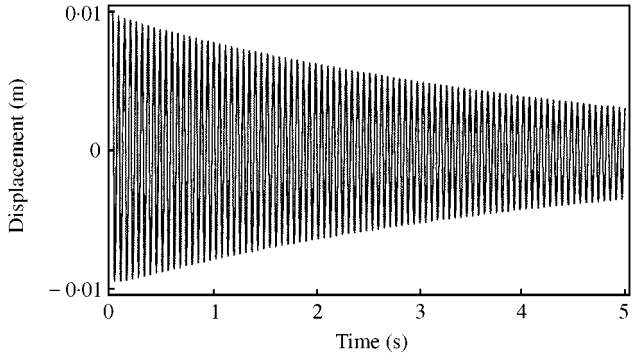

Figure 5. Free snap-back response of the plate bending mode.

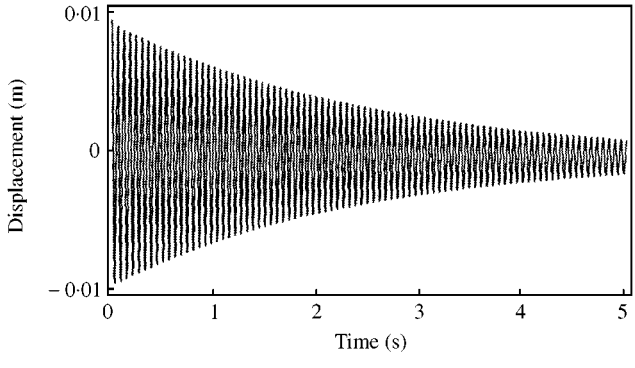

Figure 6. Controlled snap-back response.

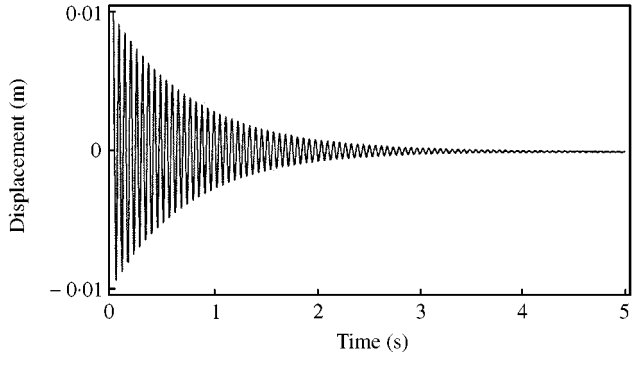

Figure 7. Controlled snap-back response (high gain).

both have identical bending control effectiveness. However, only the X-actuator configuration has the torsion control capability. Thus, redesigning the actuator layouts to the diagonal X-configuration based on the identical actuator area does enhance the torsion controllability, without loosing the bending controllability. Note that there is a gap between the last actuator patch and the fixed end in both models. Adding an extra actuator patch filling in the gap would enhance the control effectiveness, especially for bending modes.

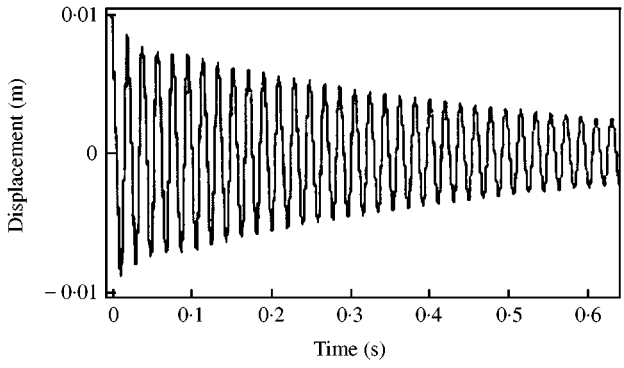

Figure 8. Free torsion vibration.

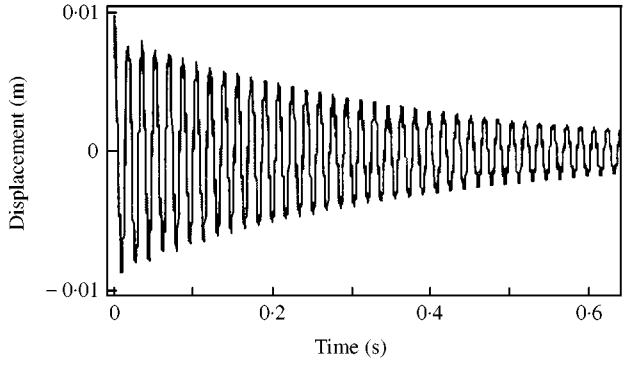

Figure 9. Controlled torsion vibration (gain $= 1\omega$).

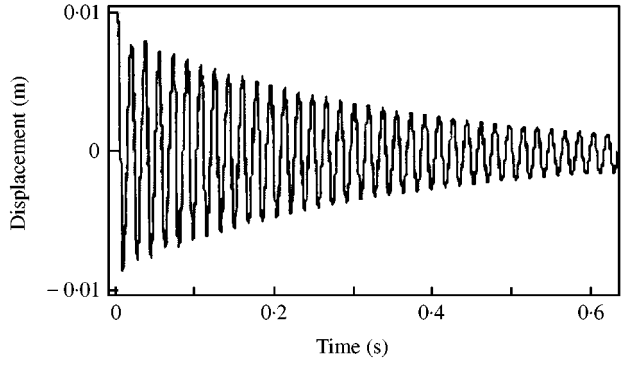

Figure 10. Controlled torsion vibration (gain $= 2\omega$).

Furthermore, spatially shaping the distributed sensors and actuators can make them sensitive to only a single mode or a group of natural modes [15–17]. Accordingly, a single critical mode or a group of modes can be independently controlled.

4. LABORATORY EXPERIMENTS

A scaled-model (10 cm × 7·5 cm × 0·5 mm) of a plexiglas plate sandwiched between two layers of piezoelectric polyvinylidene fluoride (PVDF) films (40 μm) is fabricated and its

bending/torsion control characteristics are investigated. Note that one PVDF layer serves as a distributed sensor and the other PVDF layer serves as the distributed actuator. Signal from the sensor layer is amplified and fed back to the distributed actuator layer-inducing counteracting control moments. Figure 11 shows the physical model mounted on a shaker and Figure 12 illustrates the experimental set-up and apparatus. As discussed previously, the physical model exhibits a bending mode and a torsion mode as its first two natural modes. Besides, to demonstrate the dual-mode controllability of the X-actuator, the original and controlled bending and torsion vibrations are evaluated. (Since the X-configuration has the same bending control effect as that of the parallel actuator, the parallel configuration model was neither fabricated nor tested.)

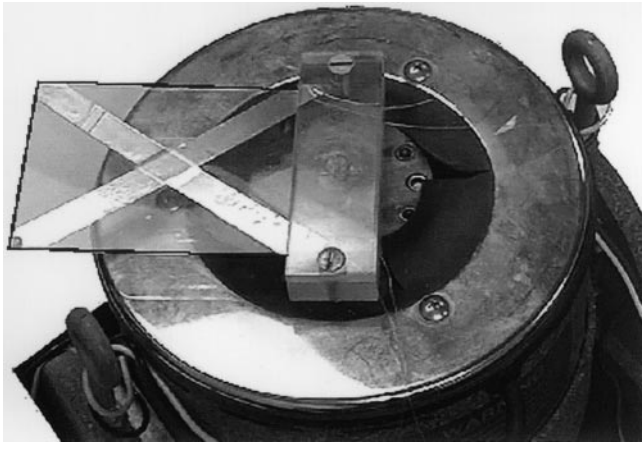

Figure 11. A physical model mounted on a shaker.

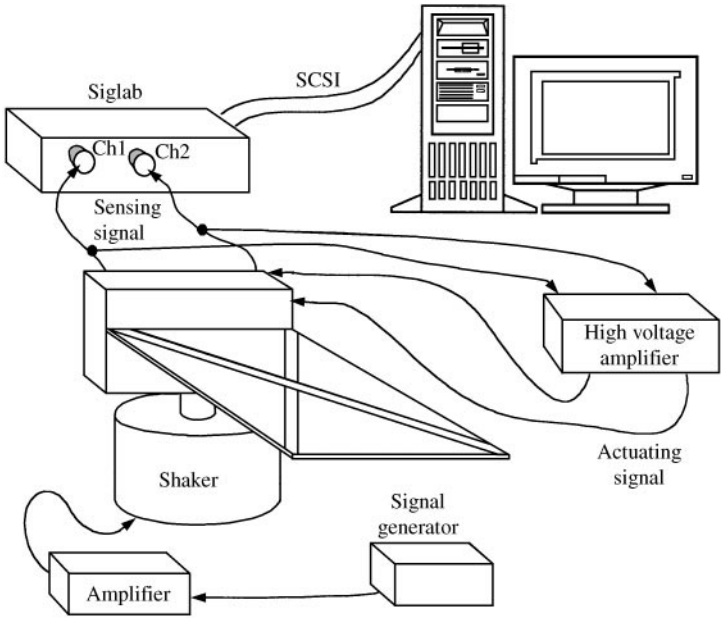

Figure 12. Laboratory set-up and apparatus.

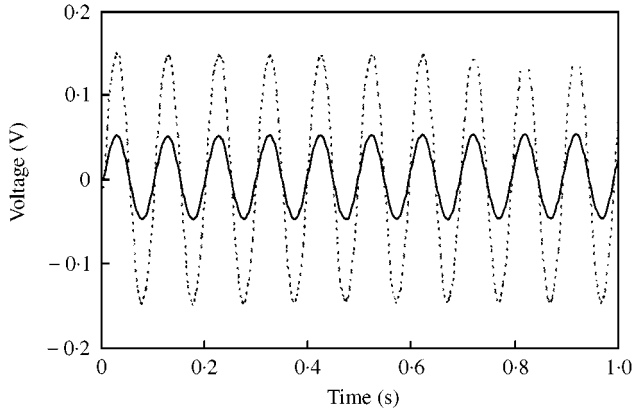

Figure 13. Steady state responses of the bending mode: (——), controlled; (- - - -), uncontrolled.

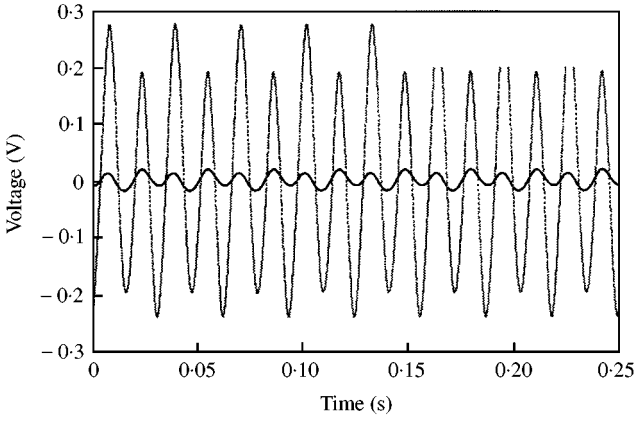

Figure 14. Steady state responses of the torsion mode: (——), controlled; (- - - -), uncontrolled.

The first plate bending mode can be easily excited using either the initial displacement (the snap-back response), the laminated PVDF actuator layer, or the shaker (the sinusoidal steady state response). However, due to technical difficulty in exciting the torsion mode via the electromagnetic shaker, the diagonally laminated PVDF is used to excite the torsion mode. An excitation signal at the torsion frequency is amplified using a high-voltage amplifier and then used as input to the diagonal PVDF actuator. Steady state responses of the controlled and uncontrolled plate time histories obtained from the PVDF sensor are presented in Figure 13 (the bending mode) and Figure 14 (the torsion mode). (Note that the initial displacement applied to the first mode was 10 mm and these vibration amplitudes were in the mm range.) These figures clearly demonstrate that diagonally laminated actuators are capable of controlling the bending and torsion modes of the plate. Also, due to imperfect fabrication techniques, the time histories also exhibit repeated waveforms of uneven torsion oscillations.

5. CONCLUSIONS

Distributed structural control based on the structronics technology has demonstrated its effectiveness in many engineering applications, i.e., airplane wings, helicopter blades, nozzles, satellites, aerospace systems, etc. Earlier studies of vibration control of airplane

wings and helicopter blades revealed that the parallel-actuator configuration is effective to control the bending modes and ineffective to control the torsion modes. Thus, reconfiguring the actuator layout, based on the same effective actuator area, capable of controlling both bending and torsion modes is highly desirable. Accordingly, the actuator patches were reconfigured into an X-actuator configuration and its bending and torsion controllability was evaluated using a newly developed finite element code and was also demonstrated in laboratory experiments.

Fundamental piezoelectric constitutive relations were briefly reviewed. Development of a laminated quadratic piezoelastic triangular shell FE using the layerwise constant shear angle theory was also presented. The governing piezoelectric matrix equation was derived and its distributed control applications were discussed. FE models of the new X-actuator configuration and the original parallel-actuator configuration were analyzed. Bending and torsion control effects of the FE models were studied. Analysis results suggested that the X-actuator configuration does provide the torsion mode controllability, while maintaining the bending mode controllability. Laboratory experiments also demonstrated the bending and torsion control effectiveness of the X-actuator configuration. Thus, effective and innovative design layouts of available distributed actuators can maximize the control effectiveness encompassing multiple vibration modes.

ACKNOWLEDGMENTS

This research is supported, in part, by a grant (F49620-98-1-0467) from the Air Force Office of Scientific Research (Project managers: Dan Segalman and Brian Sanders). This support is gratefully acknowledged.

REFERENCES

1. H. S. TZOU and G. L. ANDERSON (editors) 1992 *Intelligent Structural Systems*. Dordrecht/Boston: Kluwer Academic Publishers.
2. H. S. TZOU and A. GURAN (editors) G. L. ANDERSON; M. C. NATORI, U. GABBERT, J. TANI and E. BREITBACH (Associate Editors) 1998 *Structronic Systems—Smart Structures, Devices and Systems*, Vol. 1: *Materials and Structures*, Vol. 2: *Systems and Control*. Singapore/NJ: World Science Publishing Co.
3. H. S. TZOU and L. A. BERGMAN (editors) 1998 *Dynamics and Control of Distributed Systems*. New York: Cambridge University Press.
4. H. Allik and T. J. R. Hughes 1979 *International Journal of Numerical Methods Engineering* **2**, 151–168. Finite element method for piezoelectric vibration.
5. M. NAILON, R. H. COURSANT and F. BESNIER 1983 *ACTA Electronica* **25**, 341–362. Analysis of piezoelectric structures by a finite element method.
6. M. W. OBAL 1986 *Vibration Control of Flexible Structures Using Piezoelectric Devices as Sensors and Actuators*. Ph.D. Thesis, Georgia Institute of Technology.
7. H. S. TZOU and C. I. TSENG 1990 *Journal of Sound and Vibration* **138**, 17–34. Distributed piezoelectric sensor/actuator design for dynamic measurement/control of distributed parameter systems: a finite element approach.
8. S. K. HA, C. KEILERS and F.-K. CHANG 1992 *American Institute of Aeronautics and Astronautics Journal* **30**, 772–780. Finite element analysis of composite structures containing distributed piezoceramics sensors and actuators.
9. W.-S. HWANG and H. C. PARK 1993 *American Institute of Aeronautics and Astronautics Journal* **31**, 930–937. Finite element modeling of piezoelectric sensors and actuators.
10. S. S. RAO and M. SUNAR 1993 *American Institute of Aeronautics and Astronautics Journal* **31**, 1280–1286. Analysis of distributed thermopiezoelectric sensors and actuators in advanced intelligent structures.

11. H. S. TZOU and R. YE 1994 *American Society of Mechanical Engineers Journal of Vibration and Acoustics* **116**, 489–495. Piezothermoelasticity and control of piezoelectric systems.
12. H. S. TZOU and R. YE 1996 *American Institute of Aeronautics and Astronautics Journal* **34**, 110–115. Analysis of piezoelastic systems with laminated piezoelectric triangle shell elements.
13. R. YE and H. S. TZOU 2000 *Journal of Sound and Vibration* **231**, 1321–1338. Control of adaptive shells with thermal and mechanical excitations.
14. R. D. MINDLIN 1974 *International Journal of Solids and Structures* **10**, 625–637. Equations of high frequency vibrations of thermopiezoelectric crystal plates.
15. H. S. TZOU 1993 *Piezoelectric Shells* (*Distributed Sensing and Control of Continua)*. Boston/Dordrecht: Kluwer Academic Publishers.
16. H. S. TZOU, J. P. ZHONG and M. C. NATORI 1993 *American Society of Mechanical Engineers Journal of Vibration and Acoustics* **115**, 40–46. Sensor mechanics of distributed shell convolving sensors applied to flexible rings (PltBdTwsY.b600).
17. H. S. TZOU, J. P. ZHONG and J. J. HOLLKAMP 1994 *Journal of Sound and Vibration* **177**, 363–378. Spatially distributed orthogonal piezoelectric shell actuators: theory and applications.